Physics Letters B 761 (2016) 77–80

Contents lists available at ScienceDirect

Physics Letters B

www.elsevier.com/locate/physletb

Exploring the jet multiplicity in the 750 GeV diphoton excess

Mykhailo Dalchenko [a], Bhaskar Dutta [a], Yu Gao [a,*], Tathagata Ghosh [a], Teruki Kamon [a,b]

[a] Mitchell Institute for Fundamental Physics and Astronomy, Department of Physics and Astronomy, Texas A&M University, College Station, TX 77843-4242, USA
[b] Department of Physics, Kyungpook National University, Daegu 702-701, South Korea

ARTICLE INFO

Article history:
Received 27 June 2016
Accepted 6 August 2016
Available online 10 August 2016
Editor: J. Hisano

ABSTRACT

The recent diphoton excess at the LHC has been explained tentatively by a Standard Model (SM) singlet scalar of 750 GeV in mass, in the association of heavy particles with SM gauge charges. These new particles with various SM gauge charges induce loop-level couplings of the new scalar to WW, ZZ, $Z\gamma$, $\gamma\gamma$, and gg. We show that the strength of the couplings to the gauge bosons also determines the production mechanism of the scalar particle via WW, ZZ, $Z\gamma$, $\gamma\gamma$, gg fusion which leads to individually distinguishable jet distributions in the final state where the statistics will be improved in the ongoing run. The number of jets and the leading jet's transverse momentum distribution in the excess region of the diphoton signal can be used to determine the coupling of the scalar to the gauge bosons arising from the protons which subsequently determine the charges of the heavy particles that arise from various well-motivated models.

Both ATLAS and CMS collaborations have reported an excess of diphoton events at a reconstructed invariant mass of about 750 GeV. This excess is visible in the data at 13 TeV [1,2] and consistent with 8 TeV [3,4]. The local signal significance of the excess by ATLAS is 3.6σ for an integrated luminosity of 3.2 fb^{-1} at 13 TeV and about 1.9 σ from 20.3 fb^{-1} at 8 TeV, while the local signal significance by CMS is 3.4σ by combining results from luminosities of 3.3 fb^{-1} and 19.7 fb^{-1} at 13 and 8 TeV, respectively. It is noted that the observed significance by CMS is maximized for a narrow decay width of $\Gamma/m \leq 10^{-2}$, while the ATLAS result is in favor of a larger width with $\Gamma/m \sim 0.06$. Using the limited data, ATLAS has also reported jet multiplicity distributions in the diphoton excess region and its sidebands.

In this Letter, we point out that the jet topology could be powerful in distinguishing different models in the excess region when more data becomes available in the ongoing run.

Among numerous hypotheses [5,6] to explain the diphoton excess, we focus on the phenomenologically minimal setup by introducing a Standard Model (SM) singlet X with a mass of 750 GeV accompanied by multiplets of vector-like particles which possess SM charges. The effective coupling of SM SU(2)$_L$ and U(1)$_Y$ gauge bosons to the 750 GeV resonance can be induced at loop level by heavy new particles, as shown in Fig. 1, and can be written as

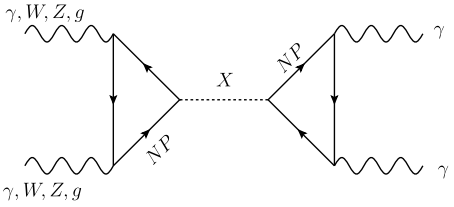

Fig. 1. Loop-induced couplings between photons and 750 GeV resonance. 'NP' denotes for any new physics heavy particles that are charged under the SM gauge groups.

$$\mathcal{L}_{\text{eff}} \supset \kappa_1 X B^{\mu\nu} B_{\mu\nu} + \kappa_2 X W^{\mu\nu} W_{\mu\nu} + \kappa_3 X G^{\mu\nu} G_{\mu\nu}. \tag{1}$$

The coupling values are determined from the heavy particles' masses and charges under the SM gauge groups. After rotations they give rise to effective couplings between X and the physical gauge bosons,

$$\begin{aligned} \kappa_{\gamma\gamma} &= \kappa_1 \cos^2\theta_W + \kappa_2 \sin^2\theta_W\,, \\ \kappa_{ZZ} &= \kappa_2 \cos^2\theta_W + \kappa_1 \sin^2\theta_W\,, \\ \kappa_{Z\gamma} &= (\kappa_2 - \kappa_1)\sin 2\theta_W\,, \\ \kappa_{WW} &= \kappa_2\,, \quad \kappa_{gg} = \kappa_3. \end{aligned} \tag{2}$$

* Corresponding author.
E-mail address: gao1yu3@gmail.com (Y. Gao).

http://dx.doi.org/10.1016/j.physletb.2016.08.012

The relative size of these couplings are among the most characteristic predictions of new physics scenarios that implement new heavy particles. For instance, Ref. [7] proposes the gauge unification under SU(6) at $\mathcal{O}(10^{16})$ GeV which require the existence of a number of new fermions which include down type SU(2) singlet vector-like quark D and vector-like SU(2) lepton doublet L. The multiplicity of these new fermions and masses fixes κ_i and subsequent X decay branching fractions into $\gamma\gamma, gg, Z\gamma, ZZ$ and WW final states. Similarly, one can introduce Q, E and U type vector-like fermions to satisfy the data in the context of $10+\overline{10}$ representation of SU(5) [8]. These are just two examples of new physics models in which the heavy particles' SM charge assignments predict the relative sizes of κ_i.

The relative strengths of κ_is not only predict the branching ratios of $\gamma\gamma$, gg, $Z\gamma$, ZZ and WW final states, but they also give us several production possibilities of X via fusion of different gauge bosons. For example, in case of larger $\kappa_{WW,ZZ}$ couplings, we expect $pp \to ZZ, Z\gamma, WW, jj$ with high p_T jets to be the primary predictions from these effective couplings. Such channels can be tested in the upcoming LHC dijet, multi-lepton, and leptons + photon resonance searches. Alternatively, in a dominant $\kappa_{\gamma\gamma}$ case we can expect less associated jets with significant p_T. Therefore, different scenarios with various values of κ_i that yield unique final state jet distributions provide us with a very promising probe of the production mechanism of the resonance.

Let us now discuss the productions of X via various mechanisms due to each κ_i and their predictions on the associated jet multiplicity and the leading jet p_T distribution.

Photon-fusion has been proposed in Ref. [9,10], and the initial state photon is studied kinematically in detail [11]. These studies differentiate the photon fusion from other, especially gluon fusion, in the photon kinematics and jet p_T. In this work, we focus on the jet multiplicity as the distinctive feature and compare with experimental data.

Photon-fusion can obtain domination with $\kappa_1 \gg \kappa_2, \kappa_3$, for example, when the mediators inside the loop are non-colored $\mathrm{SU}(2)_L$ singlets, like heavy partners of right-handed charged leptons. Their electric charge (from their hypercharge) generates photonic couplings that explain the excess, yet without inciting large couplings to the gluon or W boson.

A unique kinematic feature of inelastic photon fusion is the photon's collinear enhancement that strongly favors low p_T recoil on its parent parton, thus leads to low p_T and/or high pseudorapidity initial state jets, which prevent such jets from populating the central detector regions. Elastic photons [9,11] from the proton also make a sub-leading contribution, where photon emission is also suppressed by proton scattering p_T and would dominantly yield a jet-less final state. Comparing the number of jets, N_j in the observed η ranges from ATLAS's diphoton sample [4] can be a useful way to check whether the experimental excesses show preference to photon-fusion as the major production mechanism.

We simulated the N_j distribution with a κ_1 dominant benchmark point for the jet distributions from photon fusion. We use MadGraph [12] and the recent NNPDF23_LO set [13], which includes the photon's distribution inside the proton. Pythia [14] is used for parton shower and Delphes [15] for detector simulation. The N_j from photon-fusion is shown in Fig. 2, with jet $p_T > 25$ GeV in the pseudorapidity range $|\eta| < 4.4$, from ATLAS [4]. We consider the pile-up effects to be well-eliminated in experimental analysis and are thus not included here. To fully account for the jets from $\gamma\gamma$ fusion, we calculate both the total cross section $\sigma^{\mathrm{tot}}(\gamma\gamma \to \gamma\gamma)$ where the initial γ as a parton, and also for the one-jet process $\sigma(\gamma p \to \gamma\gamma j)$, plus subsequent showers. The latter gives the N_j distribution of one or more jets. We then add the difference $\Delta\sigma \equiv \sigma^{\mathrm{tot}} - \sigma^{ap}$, which fails to produce a jet, to the zero-jet bin. We did not include the elastic and semi-elastic contributions here, which would also dominantly fall into the zero-jet case.

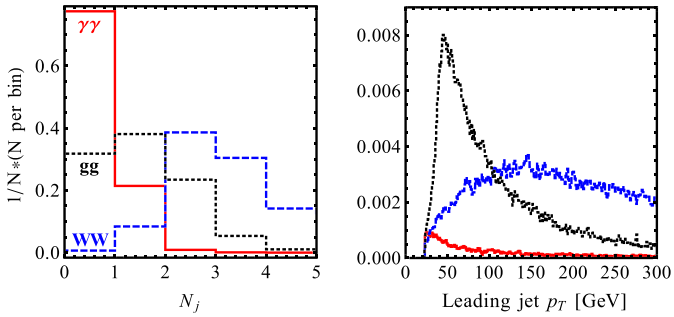

Fig. 2. Detector-level central region N_j (left) and jet p_T distribution from photon (red-solid), WW (blue-dashed) and gg (black-dotted) fusions. (For interpretation of the references to color in this figure legend, the reader is referred to the web version of this article.)

As a note, κ_1 would also enable ZZ fusion, and $\kappa_{ZZ}/\kappa_{\gamma\gamma}$ could be enhanced in the limit $\kappa_1 \to -\kappa_2 \tan^2\theta_W$, however, this condition requires a tuning of gauge group mixing and may be very model-dependent. Generally the collinear enhancement of γ emission would let $\gamma\gamma$ fusion dominate over ZZ fusion (and the mixed γZ). As ZZ is kinematically almost identical to WW fusion, we do not list it as a separate case in this work. Both $Z\gamma$ and ZZ can lead to high p_T jet(s).

WW fusion, in comparison, is present if the heavy mediators are charged under the SM's $\mathrm{SU}(2)_L$, e.g., vector-like lepton doublets, quark doublets in $5+\bar{5}$ and $10+\bar{10}$ multiplets of SU(5), etc.

Noted that with a non-zero κ_2, κ_{WW} would often coexist with $\kappa_{\gamma\gamma}$, and $WW, \gamma\gamma$ fusions would interfere. For illustrative purposes, here we choose a special case $\kappa_1 \sim -\kappa_2 \tan^2\theta_W$ to suppress $\kappa_{\gamma\gamma}$ relative to κ_{WW}, and provide a WW fusion dominated production process.

Unlike the $\gamma\gamma$ fusion case, the WW fusion always comes with two associated initial state jets (aka VBF jets) and the central jet multiplicity would peak at $N_j = 2$. Due to the weak-scale mass of the W boson, Ws are not forwardly enchanced, and a typical ISR jet would acquire $p_T \sim \mathcal{O}(M_W)$ or higher, as shown in Fig. 2. It is clear that WW and $\gamma\gamma$ fusion cases differ significantly in both jet multiplicity and jet p_T distributions.

gg fusion can be the leading production channel if heavy mediator are colored, or if X is a composite particle made of colored fields [6,16], etc. A very similar case is that X may have a small tree-level coupling $X\bar{q}q$ with quarks, if it is an $\mathrm{SU}(2)_L$ doublet. Both $gg, q\bar{q} \to X$ initial states are dominated by QCD and produce ample initial state radiation (ISR) jets. A distinction between gg and $q\bar{q}$ initial states has been pointed out in Ref. [17]. The jet multiplicity distribution will follow a power-law shape which is typical for QCD radiation, and jet p_T distribution will also show a similar behavior, as shown in Fig. 2.

In the event generation for gg fusion, we included $gg \to X$, $gp \to Xj$ and $pp \to Xjj$ processes to fully account for ISR jets. MLM matching [18] with $xqcut > 40$ GeV and $Q\,cut > 40$GeV are used to avoid double counting. Although both N_j distributions favor low multiplicity in both $\gamma\gamma, gg$ fusion, gg differs from $\gamma\gamma$ with a much less pronounced weight in the zero-jet final state. This indicates that gg fusion production has a higher fraction of signal diphoton events with ISR jet(s), whereas $\gamma\gamma$ fusion predicts much fewer associated jets in signal events. Fusion of massive gauge bosons, WW and ZZ, also predicts associated jets with p_T above their mass scale, and a different shape in the leading jet p_T spectrum, as shown in Fig. 2.